Recent Application Results from the novel e-beam based mask repair system MeRiT™ MG

Christian Ehrlich[1], Klaus Edinger*, Thorsten Hofmann*, Wolfgang Degel[1]

[1]Carl Zeiss SMS GmbH, Carl Zeiss Promenade 10, 07745 Jena, Germany
*NaWoTec GmbH, Industriestr. 1, 64380 Roßdorf, Germany

ABSTRACT

With the continuing decrease of feature sizes in conjunction with both the enormous costs for current masks and projections for future generations the area of mask repair has often been highlighted. Clearly, a viable repair methodology going forward has the potential to significantly influence and reduce production costs for the complete mask set. Carl Zeiss SMS had, in a concerted development effort with other Zeiss daughter companies, succeeded to develop and deploy a novel mask repair tool capable of repairing specifically all types of advanced masks, such as quartz binary masks, phase shift masks, EUV masks and S-FIL imprint templates. In addition to the pure technical capability of the e-beam based approach a strong emphasis has been made towards the user friendliness and automation features of the repair process as such.

Keywords: mask repair, MeRiT™, photomask, reticle, electron beam, binary mask, PSM, phase shift, automation

1. INTRODUCTION

The challenges in repairing advanced photomasks is constantly growing with the increasing complexity of the geometries on the mask, especially against the background of the employed resolution enhancement technologies, e.g. optical proximity correction, scatter bars etc. It is industry-wide acknowledged that each of the two historically employed mask repair technologies, focused ion beam (FIB) or laser based repair, are reaching fundamental limits when it comes to repair advanced masks satisfying the current and near future industry demands.

As reported in an earlier paper, a collaboration of NaWoTec GmbH, Carl Zeiss Nano Technology Systems Division and Carl Zeiss Semiconductor Metrology Systems Division had resulted in a novel electron beam based mask repair tool based on the superior capabilities of Carl-Zeiss Gemini electron beam optics [1]. Since the e-beam based mask repair tool is essentially based on a small e-beam lithography tool, the excellent resolution can be clearly understood. In addition, the high quality electron optics has the striking advantage of delivering inspection and imaging capabilities by using the system in a SEM mode. The early commercial systems are installed now for over a year in leading captive mask shops and are utilized for repairing production masks. Together with the data delivered from the application laboratory in Germany, a vast amount of process related data could be sampled over the last year, some summary of which will be presented in this paper. After a brief overview of the system itself, describing the general components of the tool and the employed processes, the main part of the paper will then discuss highlights of specific repair processes with respect to capability and reliability , as well as specific achievements in complementing the repair process as

---

[1]ch.ehrlich@smt.zeiss.com

such with automation and logistical features in order to enhance operatability against the background of the assumed higher workload that repair systems will be facing against the demands of the industry roadmaps.

2. SYSTEM OVERVIEW

Figure 1 shows an overview photograph of a MeRiT™ e-beam mask repair tool. The central part being the small footprint core unit, small cabinets for external electronics and gas delivery to each side, respectively. Inside the core units' vacuum chamber a photomask is positioned, version dependent, either semi-automatic or via a robotic handling unit onto a laser interferometer stage. Here it resides during the repair and subsequent inspection steps. After navigating to an defective area by using the supplied inspection data file from a defect inspection tool, the essential repair step can be performed. For this suitable precursor gases are injected through nozzles in very close vicinity to the incident electron beams final lens. Excited by the electrons, the precursor gas molecules adsorbed on the surface of the mask become reactive. Depending on the precursor chemistry, the reaction induced by the incident focused electron beam, will lead to either a deposition caused by fragmentation of precursor molecules or to a reaction between the adsorbed molecules and the substrate material, resulting in volatile products that exhibit the property of etching the mask absorber material. Since the reaction is confined to the very small area exposed by the electron beam, this technique allows high resolution nanostructuring. Structures with feature size well below 30nm can therefore be produced or removed in a very accurate fashion. This allows for the two different cases of either deposition of materials or removal of materials, both of which can be performed by the MeRiT™ tool sequentially and with literally zero overhead time for interchanging between the two modes of operation. This feature is one of the strongest advocates of the underlying technology, e.g. the potential to execute clear defect repair as well as opaque defect repair with the same precision and through the same operator interface. ´

The leading edge electron optical subsystem, on which the MeRiT™ is based, is complemented by a laser interferometer stage, a charge blocking unit and a multi channel gas injection system. The electron optical column is differentially pumped and for the customized repair processes operated at 1keV. It is one of the striking features of the employed GEMINI® e-beam column, with its combined electrostatic and electromagnetic immersion lens, that, at such comparatively low electron energy of 1keV, still a high current of approximately 50pA and a very small beam spot size of about 3nm can be maintained. Obviously, this low energy of the incident electrons has very positive side effects when a damage free repair process is required. Unlike with focused ion beam systems, this allows for basically unlimited imaging of the mask during pre- and post defect review, without any damage of involved structures or any transmission loss of the quartz mask substrate. This becomes especially important against the background of the higher utilization of phase-shifting masks in current semiconductor lithography.

Fig. 1: Photo of a MeRiT™ MG, the automated e-beam mask repair system

Furthermore the gas flow of the employed process gases is controlled by flow controllers, depending on the specific chemistry involved, and the delivery of the gases to the repair sites is controlled by fast switching valves located extremely close to the nozzle outlets. This close vicinity is made possible by the unique design of the GEMINI® column. The column design makes use of a ring-shaped in-lens detector for the secondary electrons and does not rely on detectors placed besides the column which might otherwise occupy the required space.

For all types of charged particle repair schemes surface charging has been of great concern. This is because the impact of any surface charge could deflect the particle beam, leading to distorted or misplaced repairs. The proprietary charge blocking method developed for and implemented in the MeRiT™ system has resulted in the complete elimination of the charging impact to the repair process. This has been demonstrated in various repair situations on challenging substrates. As an example Figure 2 shows a live image, captured with the MeRiT™ repair system, depicting a single quartz bump. It is obvious from the visual impression that even in this challenging situation no surface charging distorts the image, rather the imaging quality is good enough to exhibit any minor surface roughness.

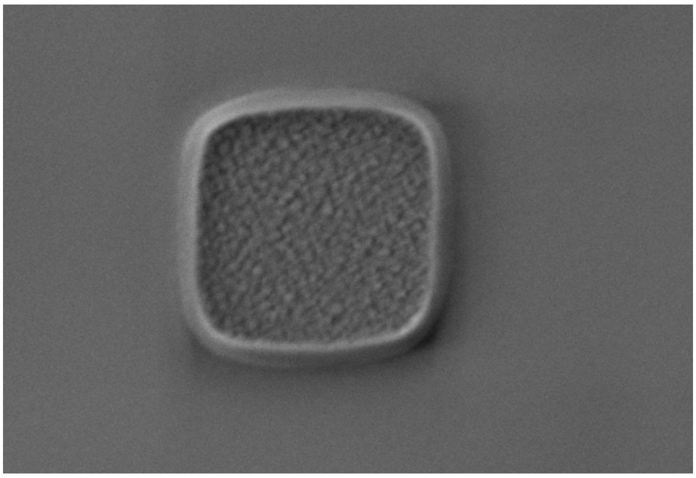

Fig. 2: Image of single quarz bump on photomask captured with MeRiT™ electron optics in repair mode

3. APPLICATION DATA

Repairs on programmed defect masks and production defects on masks have been intensively studied and evaluated on a large number of masks. The results of such studies have been reported in earlier presentations. In general the qualification of repairs performed on programmed defect masks as well as on production masks have exhibited that the resolution capabilities of the electron beam based repair tool allow for structuring, etching and depositing, of features down to sizes of 20 nanometers. Consequently, the MeRiT™ system addresses the 65nm node masks for 193nm wavelength lithography with the 45nm node masks already on the list of targets.

Picture 3 shows a synthetic repair. Here jogs of varying sizes where added to a line sub-structure. This experiment was performed in order to show the resolution capability, the placement accuracy as well as the neglectable substrate damage in e-beam based repair.

In order to verify the stability and repeatability of the discussed repair process a number of field studies were performed.

In these studies a certain type of repair was performed a number of times with varying times elapsed between the subsequent repairs. The results of the repair processes were then compared to the identical, but non-defective features on the same mask substrate. In Table No.1 the result of such a compare study is show. In this case the repair task under scrutiny was the removal/etching of defect on a chromium line on a binary mask.

Die number	Left adjacent reference space	*Left adjacent repair space*	Reference line	*Repair line*	Right adjacent reference space	*Right adjacent repair space*
1	79nm	*80nm*	80nm	*80nm*	79nm	*78nm*
2	79nm	*80nm*	80nm	*78nm*	79nm	*81nm*
3	79nm	*78nm*	80nm	*81nm*	78nm	*78nm*
4	80nm	*78nm*	80nm	*80nm*	80nm	*79nm*
5	80nm	*81nm*	80nm	*79nm*	80nm	*78nm*
Mean	79.4nm	*79.4nm*	80.0nm	*79.6nm*	79.2nm	*78.8nm*
3 sigma	1.5nm	*3.6nm*	0.0nm	*3.1nm*	2.2nm	*3.5nm*

Tab. 1: AIMS^{TM} evaluation of repaired line on binary mask critical dimension, values are on wafer level

As can be clearly seen from the respective data, the repaired line, as well as the left and right adjacent features, exhibit the same three sigma variations as does a non-defective non-repaired structure of the same geometry.

In the following Table No.2, a comparable study is shown on a phase-shifting MoSi mask. Again it is obvious from the listed values that the repair performance is extremely stable and that the achieved accuracy and 3 sigma variation is in the same order of magnitude as it is for the same pattern geometry that was not repaired.

Die number	Left adjacent reference line	*Left adjacent repair line*	Reference space	*Repair space*	Right adjacent reference line	*Right adjacent repair line*
1	78nm	*77nm*	60nm	*60nm*	77nm	*76nm*
2	80nm	*78nm*	60nm	*60nm*	78nm	*78nm*
3	80nm	*80nm*	60nm	*55nm*	79nm	*81nm*
4	78nm	*80nm*	60nm	*58nm*	77nm	*79nm*
5	78nm	*79nm*	60nm	*59nm*	78nm	*79nm*
6	81nm	*77nm*	60nm	*58nm*	78nm	*80nm*
7	78nm	*79nm*	60nm	*60nm*	79nm	*76nm*
8	77nm	*77nm*	60nm	*59nm*	76nm	*77nm*
9	79nm	*80nm*	60nm	*57nm*	78nm	*77nm*
10	77nm	*77nm*	60nm	*59nm*	76nm	*75nm*
Mean	78.6nm	*78.4nm*	60.0nm	*58.5nm*	77.6nm	*77.8nm*
3 sigma	3.8nm	*3.8nm*	0.0nm	*4.5nm*	3.1nm	*5.5nm*

Tab. 2: AIMS^{TM} evaluation of repaired space on MoSi mask critical dimension, values are on wafer level

The overall structural repair quality is shown in Picture No. 4. This image, again captured with the electron optics of the MeRiT^{TM} repair tool, shows the fidelity with which a broken line section on a phase-shifting MoSi mask could be repaired. The combined action of high quality electron optics, finely tuned precursor gas delivery, charge compensation and drift correction allows for the precise reconstruction of any missing geometry. The more practical aspects of how such accurate repair can be performed in the environment of a high end mask shop will be discussed in the next chapter.

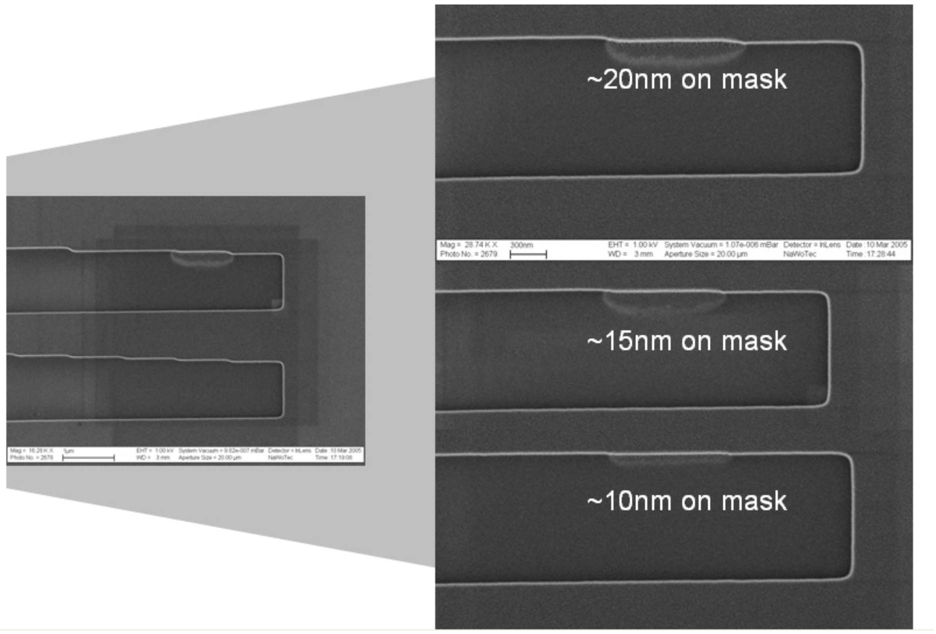

Fig. 3: Etching of jogs with varying sizes depicting ultra high resolution and accuracy

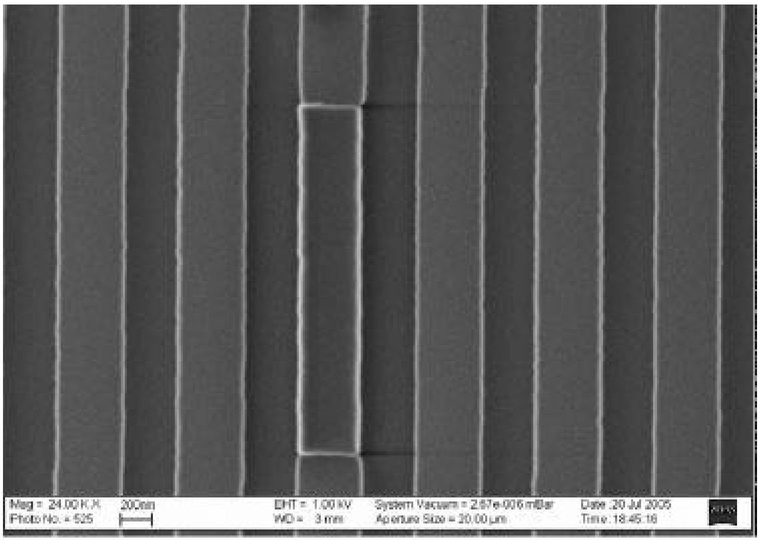

Fig. 4: Repair of broken line defect on phase-shifting MoSi mask

4. AUTOMATION FEATURES

The automated operation by means of pattern copy of the repair tool can be explained as in the following three steps:

1) navigation to the defect site and image capturing
2) employing of the pattern copy algorithms that automatically generate the missing geometry
3) the core repair procedure that physically generates the repair patch

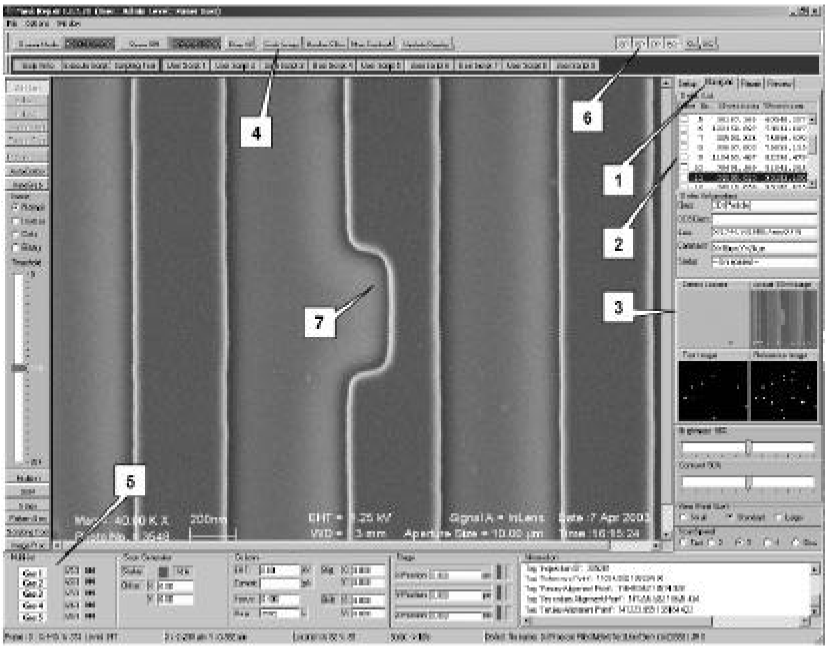

Fig. 5: Repair tool screen after navigating to defect site

In the case shown here the procedure is explained for a deposition, e.g. a clear defect repair. Nevertheless, the very same procedure is followed for any opaque defect repair as well.

In Picture 5 the main operator screen at the beginning of a repair step of the MeRiT™ is shown.

Markers 1 and 2 point at the main navigation window, where the coordinates as detected by the respective defect inspection tool can be seen. Selecting one of these defects will position the repair tool stage in such a fashion, that the defect is centered in the repair screen. Marker 3 points to the subwindow in which image processing parameters, as required by the pattern copy algorithms, can be monitored. Markers 5 & 6 point towards process module relevant parameters indicating the system status for the operator. Marker 7 indicates the defective structure.

In Picture 6 the operator screen after a successful automatic pattern copy has been achieved is shown.

Marker 1 is pointing at the automatically generated repair shape image. This calculated shape will be physically generated in the following repair step.

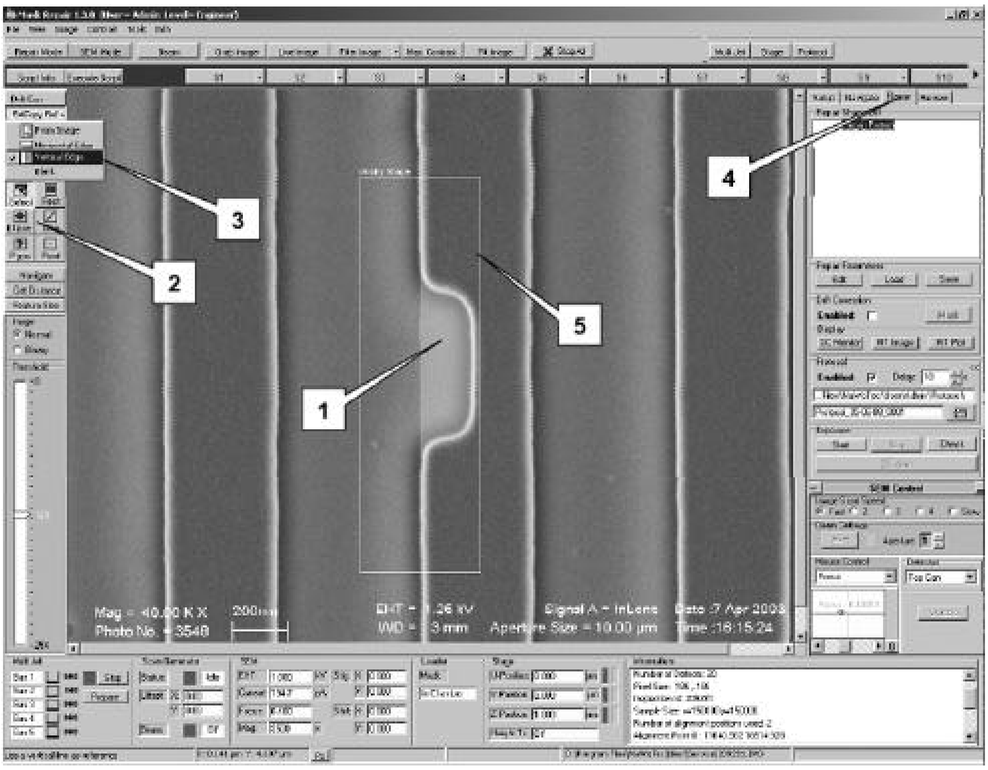

Fig. 6: Repair tool screen after pattern copy achieved

Finally in Picture 7 the operator screen after the successful repair step is shown.

This short sequence illuminates the ease of operation of a state of the art mask repair tool. The development and implementation of process modules for each specific mask and defect type has resulted in this dramatic reduction of user interference required to perform the repair tasks. This in turn allows for turnaround times for advanced mask repair which fulfill the requirements of leading edge mask shops.

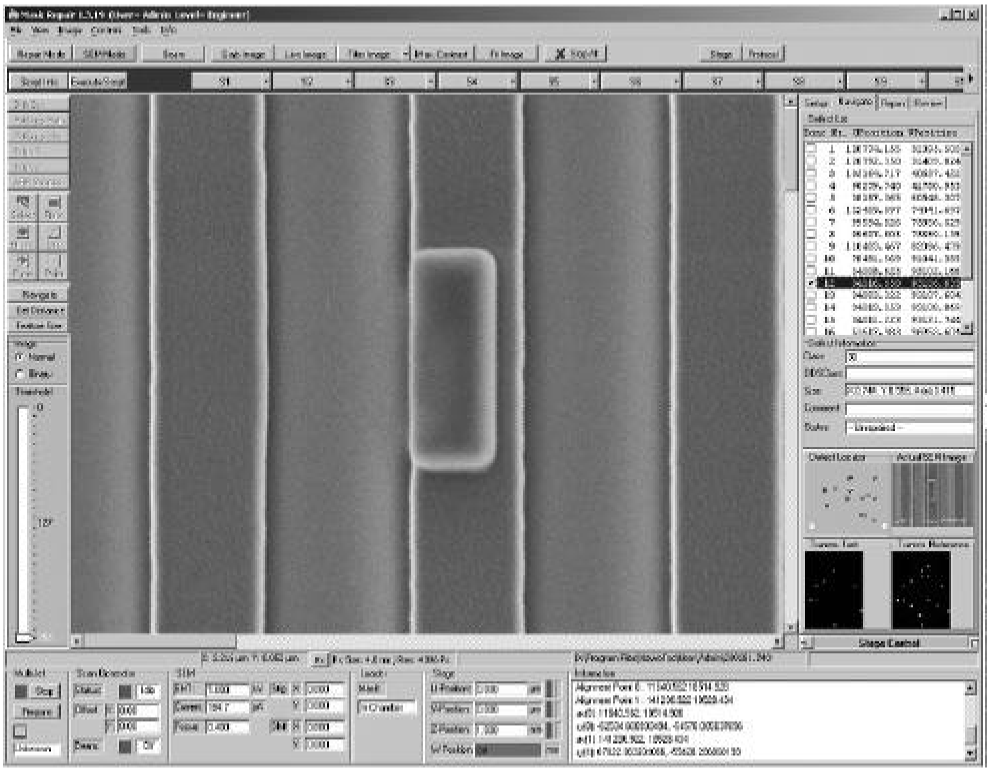

Fig. 7: Repair tool screen after successfully performed repair

5. SUMMARY

In this paper we continued the description of the electron beam based repair system MeRiT™ MG and showed application examples for electron beam induced deposition and etching. The experimental results clearly justify the current industry trend in switching to e-beam based repair schemes for the advanced photomasks for the 65nm node and beyond.

The achievable resolution of an e-beam based repair approach has been reported already earlier [2] and makes e-beam mask repair the prime candidate for mask repair not only for the 65nm node, but clearly also for the 45nm node and for EUV lithography.

REFERENCES

1. V.A. Boegli, K. Edinger, M. Budach, T. Hofmann, and J. Oster, Latest performance results from Zeiss/NaWotec MeRiT™ MG electron-beam mask repair tool", in 24th Annual BACUS Symposium on Photomask Technology, Proc. SPIE Vol. 5567, paper 5567-165,2004.
2. T. Liang, E. Frendberg, D. Bald, M. Penn and A.R. Stivers. E-beam Mask Repair: Fundamental Capability and Applications. in 24th Annual BACUS Symposium on Photomask Technology, Proc. SPIE Vol. 5567, paper 5567-49,2004